The Imaging X-ray Polarimetry Expoler mission

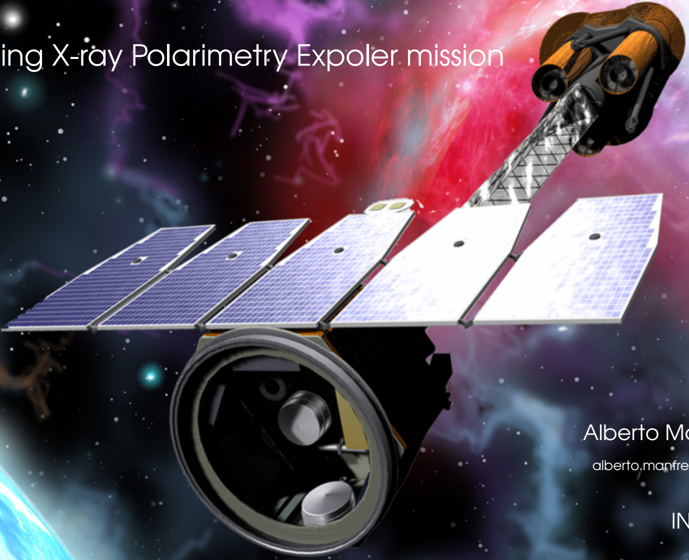

Alberto Manfreda

alberto.manfreda@pi.infn.it

INFN–Pisa

1 luglio 2020

Polarimetry in astrophysics

- Light from celestial sources can be or become polarized in many ways:
  - Non-thermal emission processes (e.g. Synchrotron radiation, Inverse Compton)
  - Scattering in aspherical geometries (matter or magnetic fields)
  - Propagating in extreme environments (e.g. vacuum birifringence at very high)
- Polarimetry provides rich information on the physics of targets that cannot be obtained in any other way:
  - Internal geometry of sources of radiation
  - Strengths and orientations of magnetic fields
  - Distribution and orientation of scattering particles
  - Fundamental physics effects (GR, QED)

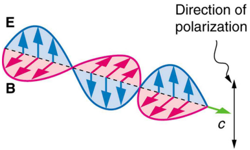

- **Polarization degree** $\rightarrow$ level and type of symmetry of the system
- **Polarization angle** $\rightarrow$ orientation.
- A single significant measurment in the soft X-ray band until today
- 20σ measurment of the Crab Nebula from a Bragg polarimeter on-board OSO-8 (1978)
- X-ray polarimetry waiting for a quantum leap. Wide space for scientific discoveries!

A turning point

letters to nature

An efficient photoelectric X-ray polarimeter for the study of black holes and neutron stars

Enrico Costa*, Paolo Soffitta*, Ronaldo Bellazzini†, Alessandro Brez†, Nicholas Lumb† & Gloria Spandre†

* *Istituto di Astrofisica Spaziale del CNR, Via Fosso del Cavaliere 100, 1-00133, Rome, Italy*
† *Istituto Nazionale di Fisica Nucleare-Sezione di Pisa, Via Livornese 1291, I-56010 San Piero a Grado, Pisa, Italy*

The study of astronomical objects using electromagnetic radiation involves four basic observational approaches: imaging, spectroscopy, photometry (accurate counting of the photons received) and polarimetry (measurement of the polarizations of the observed photons). In contrast to observations at other wavelengths, a lack of sensitivity has prevented X-ray astronomy from making use of polarimetry. Yet such a technique could provide a direct picture of the state of matter in extreme magnetic and gravitational fields[1–6], and has the potential to resolve the internal structures of compact sources that would otherwise remain inaccessible, even to X-ray interferometry[7]. In binary pulsars, for example, we could directly 'see' the rotation of the magnetic field and determine if the emission is in the form of a 'fan' or a 'pencil' beam[1,8]. Also, observation of the characteristic twisting of the polarization angle in other compact sources would reveal the presence of a black hole[9–12]. Here we report the development of an instrument that makes X-ray polarimetry possible. The factor of 100 improvement in sensitivity that we have achieved will allow direct exploration of the most dramatic objects of the X-ray sky.

The main advantage of the proposed polarimeter is its capability of investigating active galactic nuclei (quasars, blazars and Seyfert galaxies) for which polarization measurements have been suggested, crucial to understand the geometry and physics of emitting regions. We can separate synchrotron X-rays from jets[13,14] from the emission scattered by the disk corona or by a thick torus. The effects of relativistic motions and of the gravitational field of a central black hole have probably been detected by iron line spectroscopy on the Seyfert-1 galaxy MCG-6-30-15 (ref. 15) but this feature is not ubiquitous in active galactic nuclei. Polarimetry of the X-ray continuum provides a more general tool to explore the structure of emitting regions[16,17], to track instabilities and to derive direct information on mass and angular momentum[12] of supermassive black holes.

In spite of this wealth of expectations, the important but only positive result until now is the measurement, by the Bragg technique, of the polarization of the Crab nebula[18,19]. The Stellar X-ray Polarimeter[20] (SXRP) represents the state of the art for conventional methods based on Bragg diffraction and Thomson scattering. However, Bragg polarimetry[21] is dispersive (one angle at one time) and very narrow-band. Thomson polarimetry[22] is non-imaging and band-limited (>5 keV). This limits the sensitivity of SXRP to a few bright, galactic sources only.

The photoelectric effect is very sensitive to polarization. The electron is ejected from an inner shell with a kinetic energy which is the difference between the photon energy and the binding energy. The direction of emission is not uniform but is peaked around that of the electric field of the photons (see Fig. 1a). This photoelectron

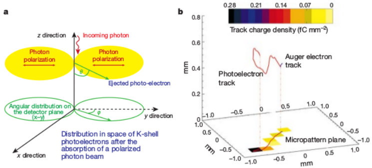

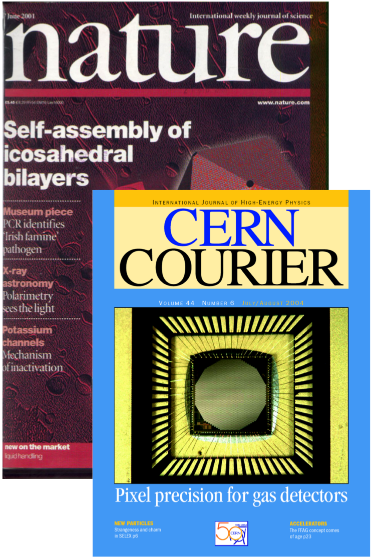

The Imaging X-Ray Polarimetry Explorer mission

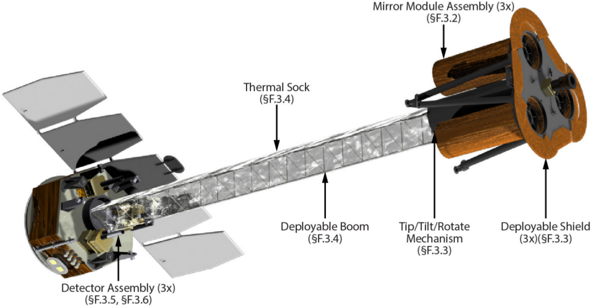

- ▷ Selected in 2017 by NASA as its next SMEX (SMall EXplorer) mission, to be launched in September 2021
- ▷ For the first time simultaneously perform imaging, spectrometry, polarimetry and timing of tens of x-ray sources
- ▷ Core technology - the focal plane detectors - is the Gas Pixel Detector: invented, developed and realized @INFN-Pisa
- ▷ 2 years of on-orbit operations + 1 years extension

IXPE science targets

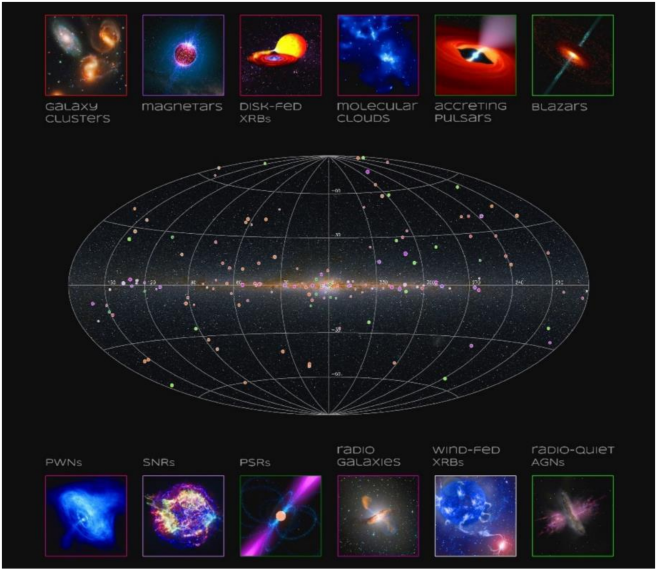

A novel view on cosmic-ray accelerators

Space resolved polarimetry

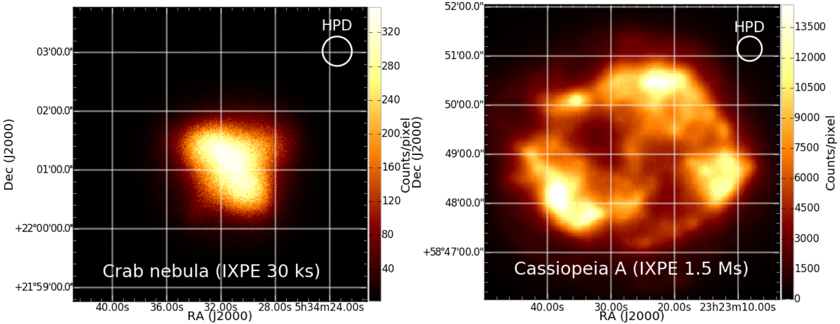

- Pulsar wind nebulæ: ordered magnetic field, high polarization degree expected
  - IXPE imaging capabilities will separate the jet and axis components
  - Will also separate pulsar from the brighter nebula emission
- Shock front in supernova remnant: candidate for comsic rays acceleration, turbolent magnetic fields
  - What is the orientation of the magnetic field at the site of acceleration?
  - How ordered is it (i.e. level of turbulence)?

Black-holes system and general relativity effects

Energy resolved polarimetry

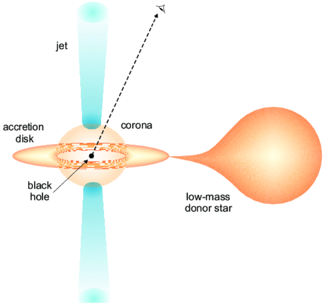

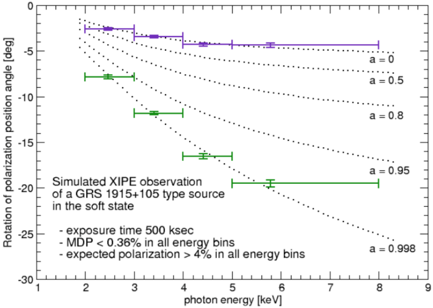

- ▷ Thermal emission from the accretion disk can become polarized (up to $\sim$ 12%) by Compton scattering on the Corona
- ▷ Including general relativity effects:
  - ▷ Black-hole proximity causes a rotation of the polarization angle;
  - ▷ Since the disk temperature decreases with the radius, the phase rotation increases with energy.
- ▷ An independet technique for measuring the black hole spin *a*

High magnetic field systems and QED effects

Phase-resolved polarimetry

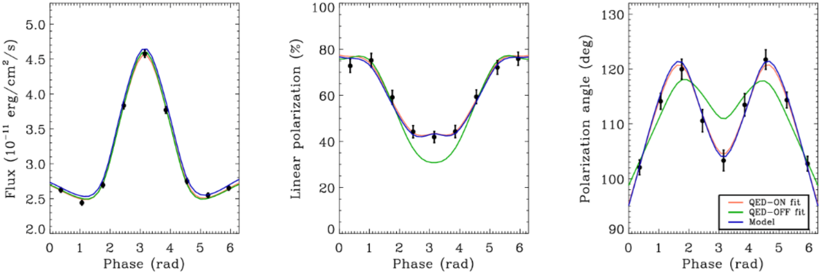

- Magnetar are ultra-magnetized neutron stars with B $\sim 10^{13}$–10^{15} G.
- In this regime the refraction index of the vacuum depends on the mangnetic field intensity:
  - Vacuum polarization, predicted by Heisenberg e Euler in 1936;

$$n_{\parallel} - n_{\perp} = \frac{\alpha_{QED}}{30\pi}\left(\frac{B}{B_{QED}}\right)^2 \sin\theta^2$$

$$B_{QED} = \frac{m_e^2 c^3}{he} = 4.4 \times 10^{13} G$$

- Negligible effect on the flux, measurable using polarimetric quantities

The spacecraft

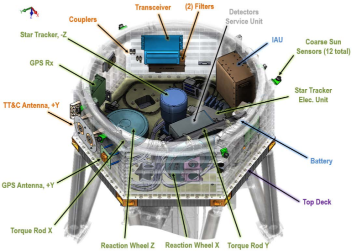

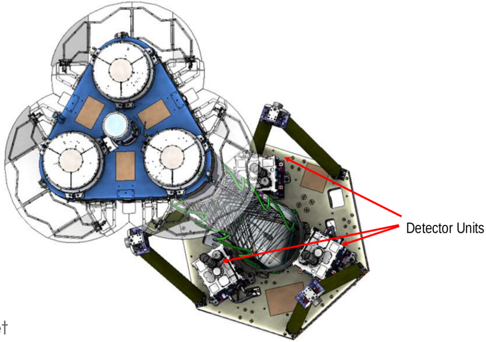

- ▷ 300 kg total mass, 200 W power budget
- ▷ Deployable boom, 4 m focal nominal length
- ▷ Originally designed to be launched from Pegasus XL, will be launched by a Space-X Falcon 9, instead
- ▷ Hosts 3 identical telescopes, each comprised of:
  - ▷ A Mirror Module Assembly (MMA) for light collection
  - ▷ A Detector Unit (DU) equipped with a polarization-sensitive detector
- ▷ DUs are rotated by 120° respect to each other (reduce systematic effets)
- ▷ A single Detectors Service Unit (DSU) on underside of deck

The Detector Unit (DU)

Exploded view

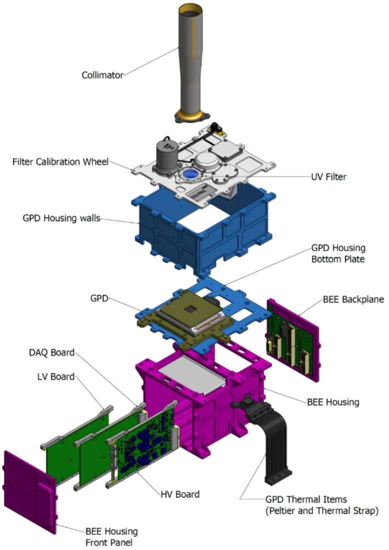

- ▷ The DU is the basic unit of the IXPE instrument
- ▷ Desing, realization and testing of the 4 Flight DUs by the INFN group
  - ▷ Including design of the Back-end electronics and DAQ firmware
- ▷ Back-end electronics mounted below the GPD on a dedicated housing
- ▷ Dedicated GPD thermal control via TEC (Peltier), heater and thermal strap
- ▷ Filter and Calibration Wheel on top of the detector for in–flight calibration and performance monitoring
  - ▷ One polarized (2 energies) and 3 non polarized sources
- ▷ Stray light collimator to block diffuse light
  - ▷ Carbon fiber and Mo (and Au) coating

The Gas Pixel Detector concept

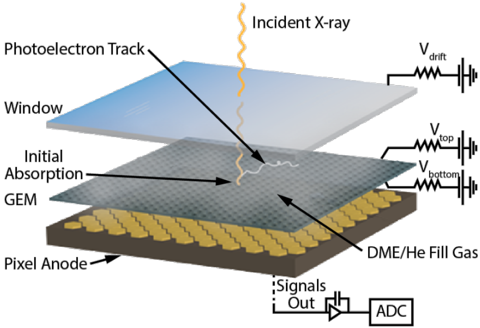

- ▷ Photoelectric effect dominant for soft (< 10 keV) X-rays
- ▷ K-shell photo-electron emission 100% modulated for linearly ploarized radiation:

$$\frac{d\sigma_C^K}{d\Omega} \propto Z^5 E^{-\frac{7}{2}} \frac{\sin^2\theta\cos^2\phi}{(1+\beta\cos\theta)^4}$$

- ▷ Typical track length ∼ µm in solid: a gaseous medium is needed!

- ▷ X-ray absorption in a gas gap
- ▷ Signal amplification via a Gas Electron Multiplier (GEM)
- ▷ Finely pixelized ASIC as readout anode
- ▷ Sensitive in the $\sim 2-8$ keV band
- ▷ Full two-dimensional imaging and spectroscopy

GPD exploded view

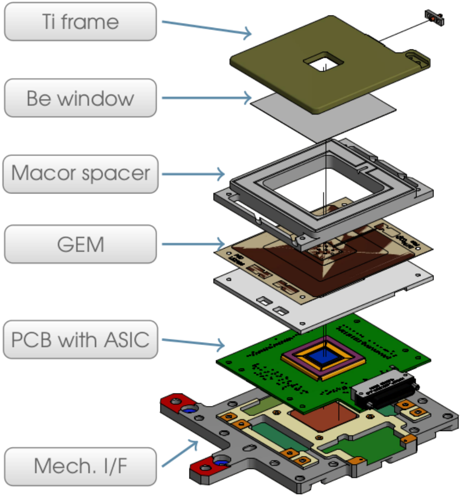

- ▷ Sealed detector, no gas system needed
- ▷ X-ray window in Be, 50 μm thick
- ▷ Gas cell thickness 1 cm
- ▷ Gas mixture DME @ 0.8 bar
  - ▷ Optimized for 2-8 keV energy range
- ▷ Transfer gap 0.6 mm
- ▷ ∼2 kV/cm drift electric field

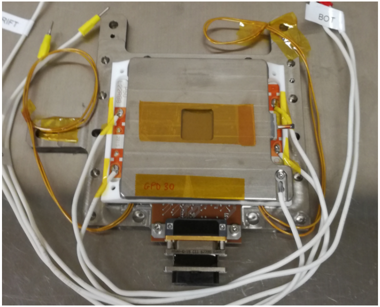

The GEM

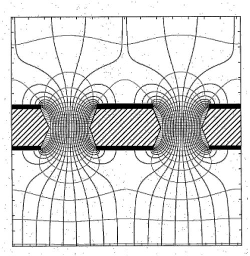

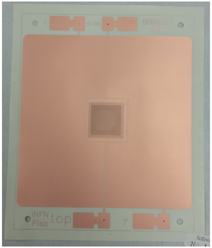

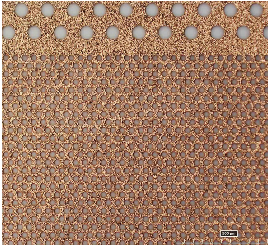

- ▷ Produced by RIKEN and SciEnergy in Japan
- ▷ 50 μm thick Liquid Crystal Polymer (LCP) insulator, 5 μm copper layer
- ▷ Hexagonal hole pattern, with 50 μm pitch, diameter of 30 μm
- ▷ Pushing the technology to its limits
- ▷ Production process refined iteratively with input from our test
  - ▷ photo-lithographic copper etching
  - ▷ CO_2 laser drill in the insulator
  - ▷ wet etching to cleanup

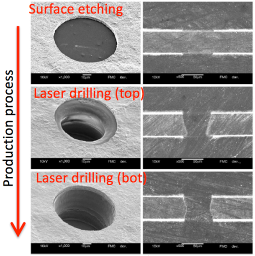

The readout ASIC

Bellazzini et al., NIM A **535**, 477–484 (2004)

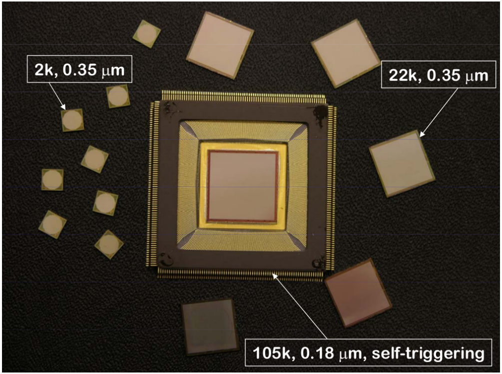

Technology	CMOS 0.18 μm
Active area	$\sim$ 15 $\times$ 15 mm
Fill factor	92 %
Number of pixels	300 $\times$ 352
Pixel pitch	50 μm
Pixel density	$\sim$ 470/mm 2
Pixel noise	$\sim$ 20 ENC
Shaping time amplifiers	3 - 10 μs
Readout clock	typically 5 MHz
Dead time	$\sim$ 1 ms

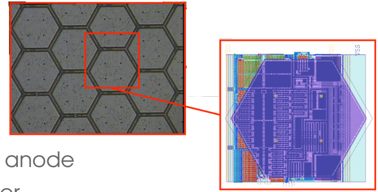

- ▷ Self-triggering, with ROI definition
- ▷ Metal top layer acting as a charge collecting anode
- ▷ Integrating preamplifier, shaper, S/H, multiplexer
- ▷ Serial readout via external 14 bits ADC

Event reconstruction

A typical 5.9 keV track (Fe55)

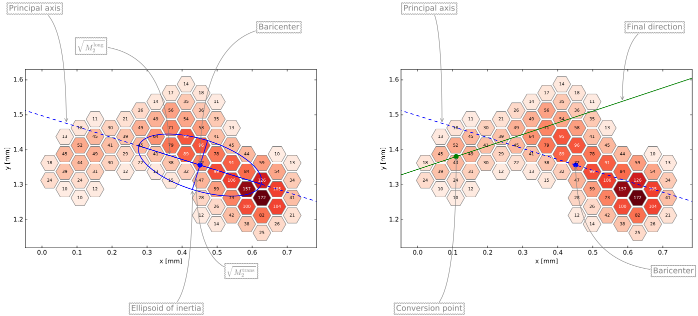

- Clustering stage to identify main track
- Moments analysis to get the ellipsoide of inertia of the charge distribution
- Exploit the Bragg peak to identify conversion point
- A second, weighted moments analysis, to improve direction estimate (especially helpful for high-energy events)
- Further imporvements using ML techniques currently at study

GPD production

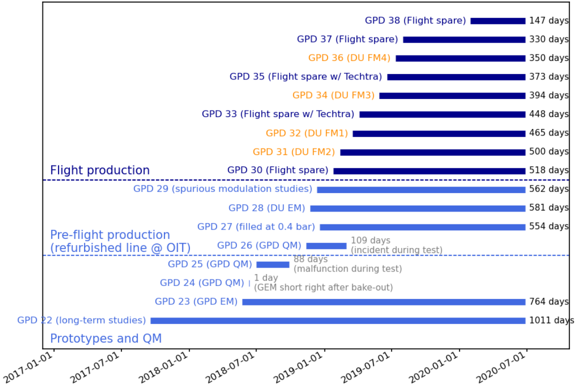

- Starting from November 2017 GPD production moved from Oxford Instrument to INFN
- Hard challenge, due to strict time schedule
  - Less than 3 years from mission approval to delivery of the last DU
- 17 GPDs: 9 FMs, 4 QM, 4 EM. 3 FMs (+1 spare) selected for the mission

GPD Assembly

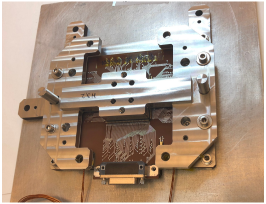

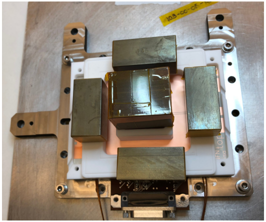

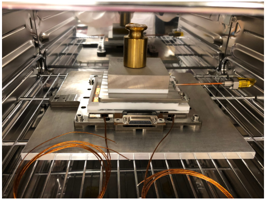

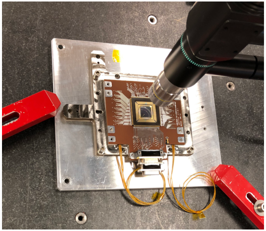

- Parts procured from external vendors or INFN-workshop
  - With INFN design
- Assembly in our clean-room.
  - Several gluing steps ($\sim$ 1 day each), some of them under CMM
- Metrology performed to verify assembly and ASIC reference system
- Electrical tests are performed during the assembly

GPD Filling and testing

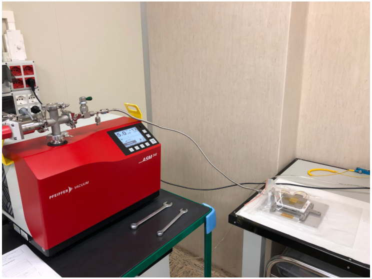

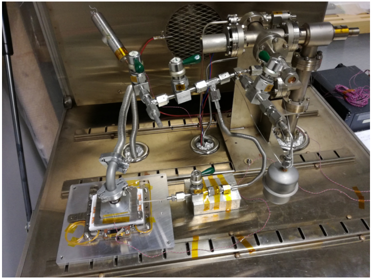

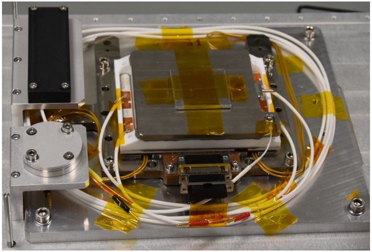

- Final leak test with He at INFN-Pisa
  - Requirement on leak rate: $< 1 \cdot 10^{-9}$ mbar l/s
- Bake-out and filling at Oxford Instrument (OIT) in Finland
  - A 2 weeks bake-out at 100 °C
  - Filling with DME at 0.8 bar is done in the same facility
  - Finally GPD is permanently sealed by crimping the filling tube
- Acceptance test done in Pisa and at IAPS

Testing the GPD with x-ray beams

Calibration facility at INAF in Rome

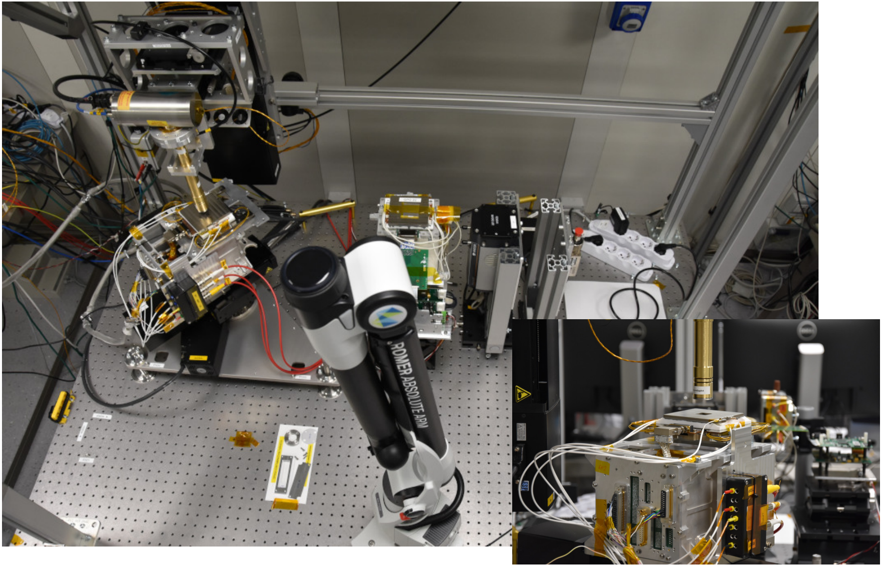

DU FM integration

All done in INFN-Pisa clean room

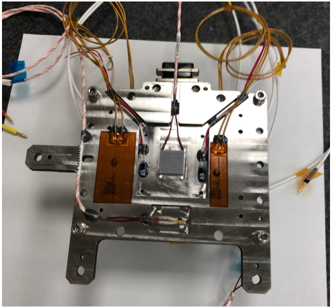

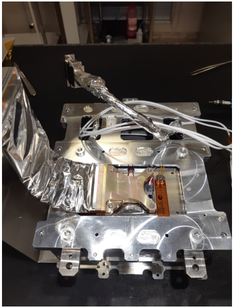

- ▷ Thermal items (heaters, sensors, TEC) gluing
- ▷ GPD cabling (support by Aviotec)
- ▷ Thermal strap integration
- ▷ Back-plane integration
- ▷ Cable routing
- ▷ BEE boards integration
  - ▷ FPGA firmware completely developed by INFN
- ▷ FCW, UV filter and collimator integration

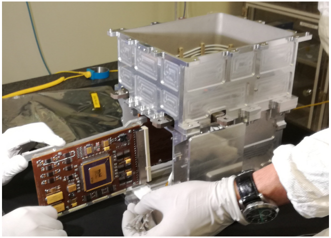

DU FM tests

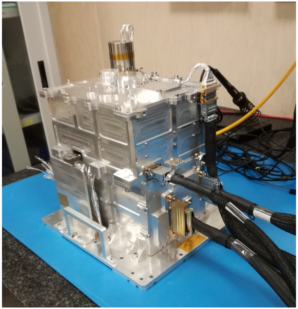

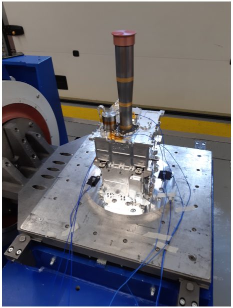

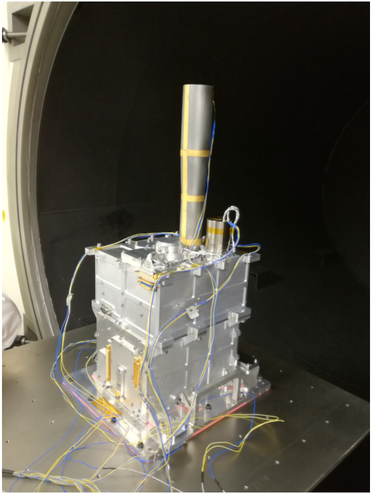

- Full Functional Test at INFN-Pisa
- Precise metrology at INFN-Pisa
- Vibration test at BPS (FM1) and SERMS
  - Followed by a functional test
- TVAC test at IAPS
  - 1 cycle at survival level
  - 7 cycles at operative levels
  - 4 cycles orbit-like to check GPD thermal control

Performance of the GPD

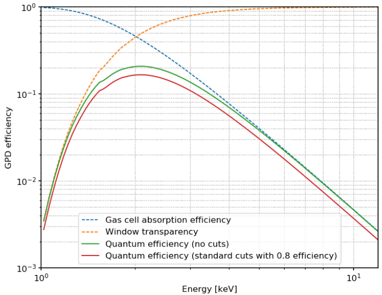

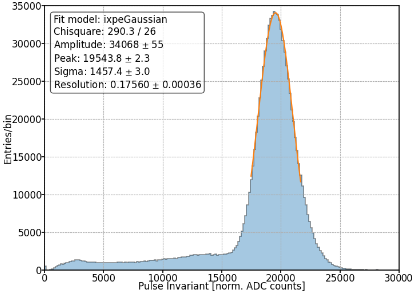

- Quantum efficiency: 20% (3%) at 2.7 keV (5.9 keV)
- Energy resolution: $\sim$ 17% at 5.9 keV.
  - Better than our mission requisite (25%)
  - Enough to perform energy-resolved polarimetry in a few bins
  - Left tail: photons converting in GEM or Be window
- Spatial resolution: $\sim$ 90 μm at 5.9 keV
  - Subdominant compared to the blurring introduced by the optics
- Temporal resolution: $\sim$ a few μs.
  - Allows phase-resolved polarimetry for pulsars

Digression - basic polarimetry formalism

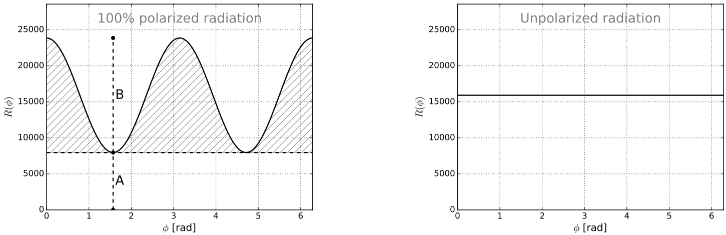

- A polarimeter essentially measures the azimuthal modulation around the polarization direction ϕ_0 of the incident photon beam:

$$R(\phi) = A + B\cos^2(\phi - \phi_0)$$

- Modulation factor: Response to 100% polarized radiation

$$\mu = \frac{R_{\max} - R_{\min}}{R_{\max} + R_{\min}} = \frac{B}{B + 2A}$$

- Minimum Detectable Polarization (MDP):

$$MDP_{99\%} = \frac{4.29}{\mu\sqrt{N}}$$

Performance of the GPD

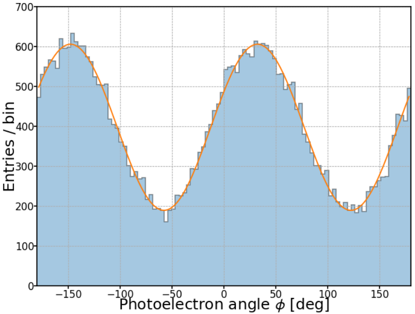

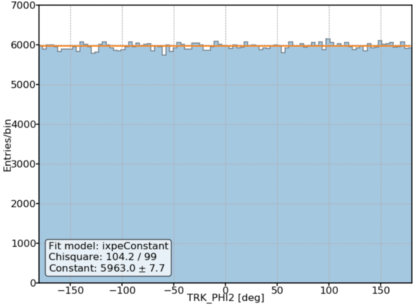

- Modulation factor: 0.3 (0.55) at 2.7 (6.4) keV.
  - Fully meet scientific requirements
- Flat response to unpolarized radiation at 5.9 keV
- What about lower energies?

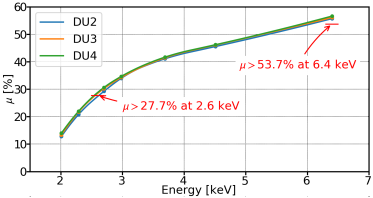

The spurious modulation puzzle

A critical moment

- One of the most delicate moment of the mission was the discovery of a spurious modulation signal during tests with low-energy pencil X-ray beams
  - Orientated vertically ($\sim 90^\circ$)
  - Effect quickly decrease with energy; $\sim$ 10% at 2.7 keV, essentially absent at 5.9 keV
  - Large variations on relatively small (sub-mm) spatial scales: virtually impossible to calibrate given the time constraints
  - Extremely resilient to changes in the hardware configuration and data processing software (e.g., gain equalization, thresholds)

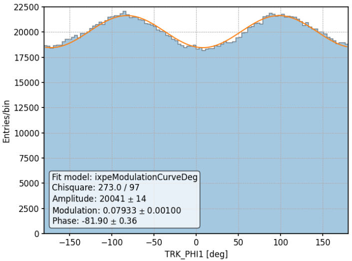

- Huge effort into understanding and solving the issue
- Purposedly filled a GPD at half pressure to see if longer tracks were less affected (they were not)

The spurious modulation puzzle

The role of the ASIC and the GEM

- We found out that part of the spurious signal was induced by coherent noise effects in the ASIC
  - Likely caused by an electrical interplay bewteen the signal and the trigger (which has its own readout chain)
  - Predictable patterns and pretty much independent from everything: easy to correct on an event-by-event base
- Note: these are effects of the order of just 2-5 ADC counts - that translates into less than 10 e^-!
- However, the spatial-dependent component was eventually attributed to the GEM
  - Laser drillling performed in separate sweeps with 1.8 mm pitch and 100 μm overlap between adjacent passes
  - Clear imprinting of the process on the GEM surface and perfect match with the spurious modulation structures

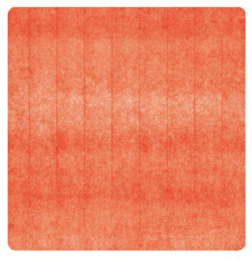

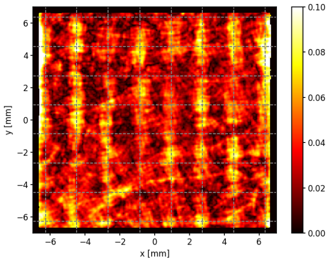

The spurious modulation puzzle

Testing different GEMs

- A different GEM producer tested (Techtra)
- Etching instead of laser drill
- Spurious modultion patterns different (and somehow better on average),
- Spatial variations still present
- Eventually sticking with SciEnergy GEMs

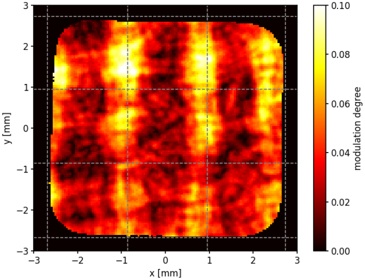

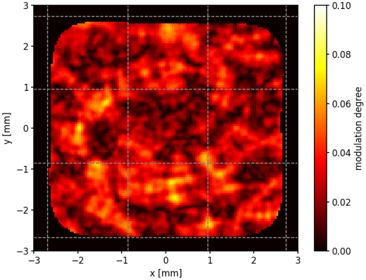

- Open problem for future missions...

The spurious modulation puzzle

Dithering

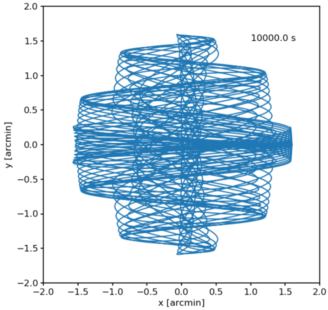

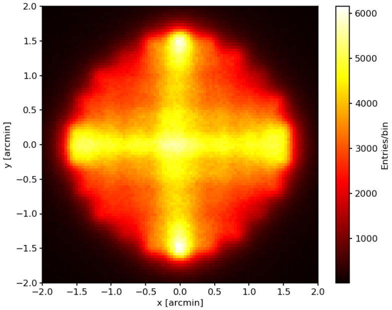

- ▷ Dithering of the Observatory along the line of sight
  - ▷ Decrease the average modulation amplitude (partial cancellation due to phase incoherence)
  - ▷ Make it possible to calibrate the rest of the effect

The spurious modulation puzzle

Final results

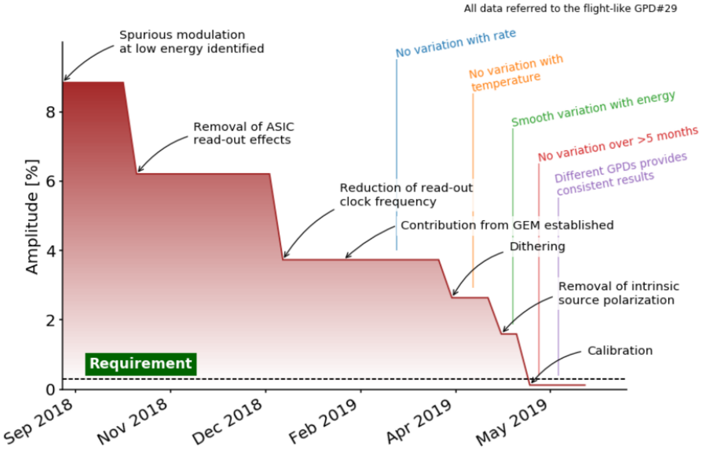

Another surprise

- ▷ Since a decade ago, it was observed that the gain of all the detectors showed a slow increasing trend over time
- ▷ Named '**secular gain variation**', as the timescale of the effect is of the order of several months
- ▷ Less compelling evidence that the modulation factor increased as well
- ▷ Initially attributed to some unknown kind of aging of the gas
- ▷ Only at the beginning of this year we discovered that what was really happening was a **pressure** decrease
- ▷ The effect manifests itself in several ways:
  - ▷ The gain increases
  - ▷ The quantum efficency decreases
  - ▷ The electron range increases (as 1/p)
  - ▷ The transverse diffusion also increases (as $1/\sqrt{p}$)
- ▷ Definitely not a leak
  - ▷ Energy resolution does not worsen (the gas stays clean)
  - ▷ Heating a GPD restores to a great extent the nominal pressure
- ▷ The gas must be adsorbed by the material - microscopic effect yet to be identified

Fitting the pressure model

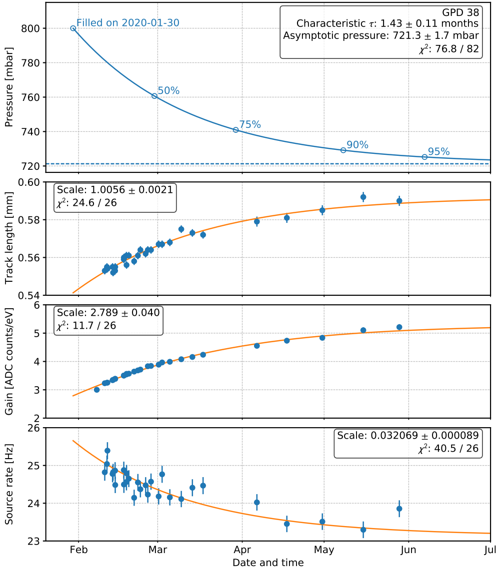

- A single model (derived from first principles and Monte Carlo simulation of the detector) fits well the three trends at the same time
- Asymptotic pressure decrease $\sim$ 100-150 mbar (over the initial 800 mbar), will saturate before launch
- Time constant varies significatively among the GPDs, from 1.5 to 15 months
- Impact on detector sensitivity much mitigated by the interplay from efficiency and modulation factor
- Impact on detector calibration: need to extrapolate from measured values

Status and Conclusions

- IXPE will open a new observative window on the Universe
- Expected to observe for the first time X-ray polarization in the soft X-ray band (2-8 keV) for many tens of sources
- Sensitivity increased by two order of magnitude compared to predecessors
- GPD detectors, invented designed and assembled at INFN (Pisa), are the core technology of the IXPE mission
- Production of flight hardware completed, instrument (3 DU FM + DSU FM) sent to Ball for integration on the spacecraft
- DU FM1 (spare) retested after undergoing a rework
  - Sent to IAPS for calibration
  - Will be used for mirrors calibration at MSFC at the end of the summer
- Launch scheduled in September 2021. . . (Covid-19 aside...)!

The IXPE team

BACKUP SLIDES

Mirror modules

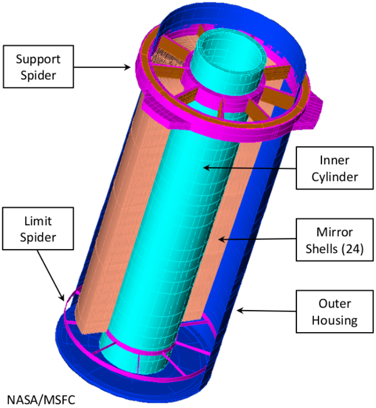

Property	Value
Number of MMAs	3
Mirror shells per MMA	24
Focal length	4000 mm
Shell length (P+S combined)	600 mm
Inner–outer shell diameter	162–272 mm
Inner–outer shell thickness	0.18–0.26 mm
Shell material	Nickel–Cobalt alloy
Mass per MMA	30 kg (current best estimate)
Effective area per MMA	210 cm^2 (2.3 keV) > 230 cm^2 (3–6 keV)
Angular resolution	≤ 25 arcsec HPD
Field of view (detector-limited)	12.9 arcmin

Mirror modules assembly

Mandrel fabrication

1. Machine mandrel from aluminum bar
2. Coat mandrel with electroless nickel (Ni–P)
3. Diamond turn mandrel to sub-micron figure accuracy
4. Polish mandrel to 0.3-0.4 nm RMS
5. Conduct metrology on the mandrel

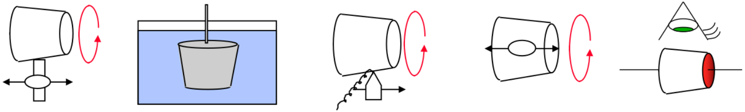

Mirror-shell forming

6. Passivate mandrel surface to reduce shell adhesion
7. Electroform Ni–Co shell onto mandrel
8. Separate shell from mandrel in chilled water

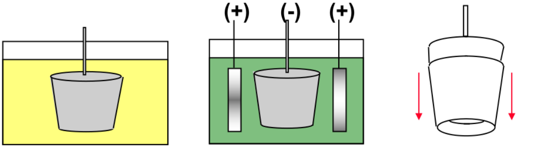

Ni–Co electroformed mirror shells

Conventional X-ray polarimetry techinques

—Bragg diffraction at 45°

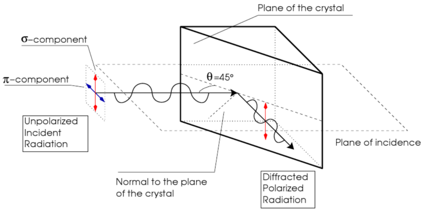

- ✓ Excellent modulation factor.
- ✓ Energy-resolved (discrete harmonics).
- ✘ Limited to low energies.
- ✘ Low efficiency (narrow band-pass).
- ✘ Dispersive (one angle at a time).
- ✘ Needs rotation.

—Thomson scattering around 90°

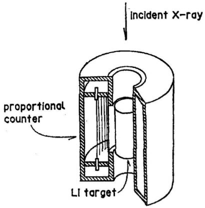

- ✓ Suitable for hard X-rays.
- ✓ Decent efficiency and modulation factor.
- ✓ Decent energy resolution.
- ✘ Limited at low energy.
- ✘ Background can be important.
- ✘ Rotation to reduce systematics.

X-ray polarimetry

"State of the art"

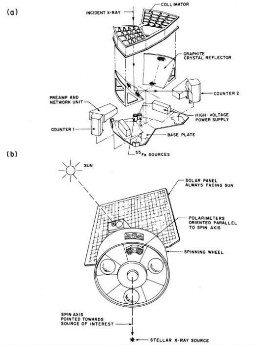

FIG. 1.—(*a*) Exploded view of the OSO-8 polarimeter assemblies. (*b*) Location of the polarimeters in the satellite.

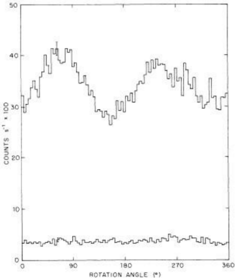

FIG. 2.—Average modulation curves obtained with both detectors at 2.6 keV during (*upper curve*) observations of the Crab Nebula and during (*lower curve*) observations of the Earth-occulted instrumental background.

- A single significant measurment in the soft X-ray band until today:
  - Weisskopf et al., ApJ **220**, 1978 (L117)
  - 20σ measurment of the Crab Nebula from a Bragg polarimeter on-board OSO-8
  - P = (19.2 ± 1.0)% at a position angle of $(156.4 \pm 1.4)^\circ$
  - Caveat: this is **linear** polarization (I will always assume that in the following)
- X-ray polarimetry waiting for a quantum leap. Wide space for scientific discoveries!

The IXPE mission

Overview

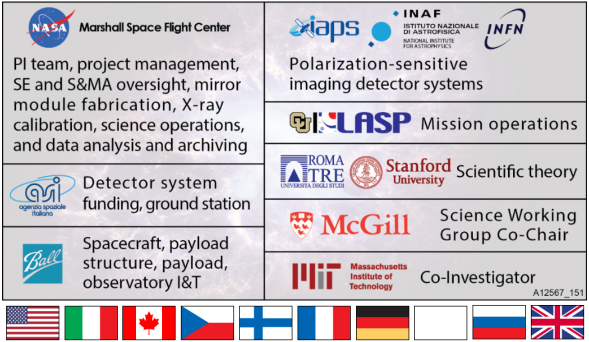

- ▷ 2 years of on-orbit operations + 1 years extension
- ▷ Point-and-stare observation mode towards predefined targets
  - ▷ Long duration - from days to week(s)
  - ▷ Data are made public after validation
  - ▷ No-repointing, but Targets of Opportunity possible in a few days
- ▷ Equatorial orbit (0.1°inclination), 600 Km nominal altitude
  - ▷ Minimize charged particle background
  - ▷ $\sim$ 13% off-time due to South Atlantic Anomaly

INFN team contribution

- Desing and realization of the Gas Pixel Detectors and associated thermal control
- DU mechanical and thermal design and parts procurement
- DU assembly and flight qualification (TVAC, EM, vibrations)
- DU alignment system design in collaboration with MSFC and Ball
- Stray-light collimator design and procurement
- BEE Electronics:
  - design, requirements specification, procurement and prototyping
  - DAQ firmware
  - Test Equipment (ITE) boards and software for performance verification
- Scientific analysis and software:
  - Event reconstruction algorithm
  - Monte Carlo simulation of the detectors
  - Celestial sources observation simulation
  - Lab DAQ software
  - Prominent contribution to ground pipeline and data analysis software tools development

Polar Light

The X-ray polarimetry window reopens

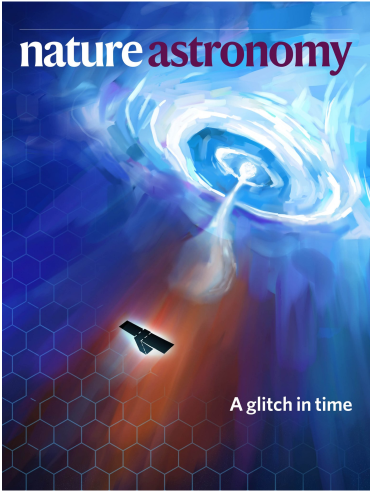

- Demonstrative mission PolarLight (on CubeSat, without optics) succesfully proved the detector concept works in space enviornement

GEM testing

- Thorough electrical and performance testing of each production batch performed in Pisa
- Dedicated set-up, reproducing the detector environement (ASIC + DAQ) with fluxed Ar/CO_2 gas mixture
- Asserting gain unformity, gain stability, etc...

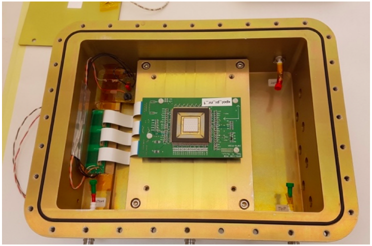

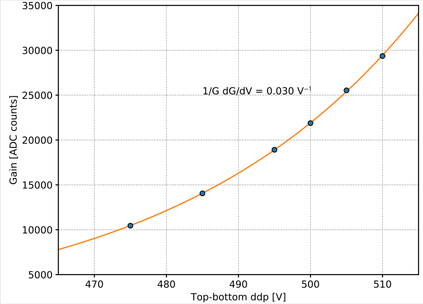

- Typical operating voltages 400 - 500 V
- Effective gain ∼200 (including collection efficiency)
- Experimental data well in agreement with simple exponential gain model

$$\frac{1}{G}\frac{dG}{dV} = \gamma \quad [V^{-1}]$$

ASIC layout

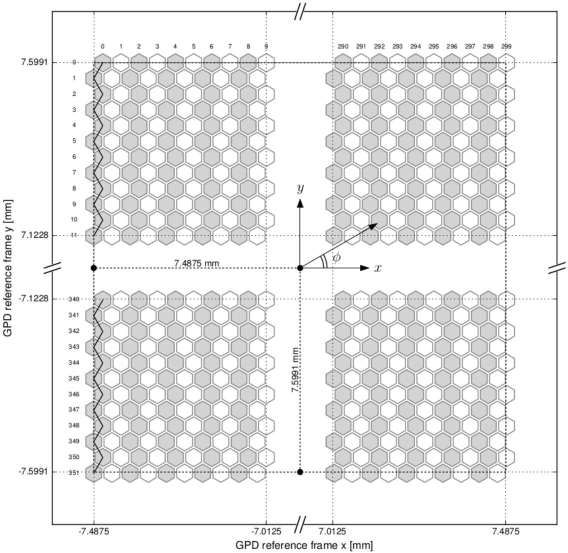
0
1
2
3
4
5
6
7
8
9
290
291
292
293
294
295
296
297
298
299
7.5991
7.1228
-7.1228
-7.5991
10
11
340
341
342
343
344
345
346
347
348
349
350
351
7.4875 mm
7.5991 mm
y
x
ϕ
-7.4875
-7.0125
7.0125
7.4875
GPD reference frame x [mm]
GPD reference frame y [mm]

ROI example

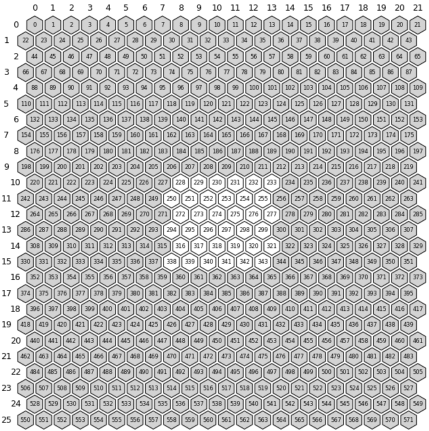

- ▷ 22×26 ROI, with trigger and padding regions highlighted